

# Large-Scale Alignment of ABC Block Copolymer Microdomains via Solvent Vapor Treatment

Kenji Fukunaga, Hubert Elbs, Robert Magerle, and Georg Krausch\*

Lehrstuhl für Physikalische Chemie II, Universität Bayreuth, 95440 Bayreuth, Germany

Received July 1, 1999

**ABSTRACT:** We have studied the microdomain morphology of thin ABC triblock copolymer films supported by a solid substrate. The films were exposed to various solvent vapors, and the effect of the solvent removal speed on the resulting morphologies is investigated. Slow solvent extraction rates lead to a parallel alignment of lamellar microphases within the plane of the film. On fast drying, a perpendicular orientation of the lamellae is found. In the case of block copolymer samples with a highly anisotropic macroscopic shape, the microdomains can be aligned over large lateral areas. The results are discussed in view of the mechanical strain fields present during the drying process.

## Introduction

Block copolymers present an interesting class of materials mainly due to their potential to self-assemble into highly regular structures of mesoscopic dimensions. The interplay of a frequently occurring incompatibility between the constituent blocks and the fact that they are covalently connected on a molecular level give rise to a rich variety of ordered microdomain morphologies in thermal equilibrium.<sup>1,2</sup> In some cases, thermodynamic equilibrium can simply be achieved by vacuum annealing above the glass-transition temperature. In many complex copolymer systems, however, the narrow temperature window between the glass-transition and the thermal degradation temperature does not suffice to achieve thermodynamic equilibrium within reasonable annealing times. Moreover, complex metastable morphologies may form during sample preparation, which in turn can constitute severe kinetic barriers for the chain transport necessary to achieve the thermodynamic equilibrium morphology. These problems generally increase with increasing molecular weight and increasing complexity of the molecular architectures. Therefore, drying from or swelling in nonselective solvents has become a prominent alternative route for block copolymer “equilibration”. Despite its widespread use, the details of this treatment remain rather unclear, and the achievement of the true melt equilibrium situation quite often remains questionable.<sup>3,4</sup> This is because truly nonselective solvents are rarely found for real block copolymer systems and solvent selectivity can have severe effects on the resulting block copolymer morphologies.<sup>5</sup> Moreover, the volume of the samples decreases on drying, which in turn will lead to undesired changes in the resulting morphologies. Finally, the experimental parameters governing the drying/swelling procedure (partial pressure of solvent, amount of solvent uptake, rate of solvent extraction, etc.) are difficult to control, imposing problems for the reproducibility and a theoretical modeling of the experimental procedure.

In the present work, we explore the effects of solvent vapor swelling and subsequent drying on the domain morphology in thin ABC triblock copolymer films. High-molecular-weight triblock copolymers are typical ex-

amples of polymeric systems where thermal treatment is not a feasible route to achieve thermal equilibrium.<sup>6</sup> We shall give indications for surface-induced microdomain alignment similar to the situation known from symmetric diblock copolymer thin films.<sup>7,8</sup> In addition, we shall show that strong internal strain fields accompanying the drying process strongly influence the observed microdomain morphologies. We shall also demonstrate that controlled solvent extraction rates together with a suitably chosen macroscopic sample geometry can be used to create highly anisotropic block copolymer monodomains.

## Experimental Section

For our experiments, we used a poly(styrene-*b*-2-vinylpyridine-*b*-*tert*-butyl methacrylate) triblock copolymer synthesized via anionic polymerization<sup>9</sup> ( $M_w = 293\,000$ , volume fractions  $\varphi_{PS} = 0.18$ ,  $\varphi_{P2VP} = 0.39$ ,  $\varphi_{PtBMA} = 0.43$ ). After slow drying from tetrahydrofuran (THF) solution, bulk pieces of the material were shown to exhibit a lamellar morphology.<sup>10</sup> Thin films of the material were deposited onto a polished Si wafer by spin casting from THF solution. Alternatively, a drop of THF solution was placed onto a Si wafer and covered by a microscope cover slide. On drying, the solution dewets the two boundary surfaces, and an interconnected system of narrow rims, reminiscent of late-stage dewetting patterns,<sup>11</sup> is formed. After drying, the top glass slide was removed for further treatment and investigation. The samples were exposed to the saturated vapor of different solvents in a closed vessel kept at room temperature. For fast drying, the samples were removed from the vessel quickly and brought in contact with a hot plate kept at 60 °C. For slow drying, small holes were punched into an Al foil covering the vessel, and the solvent was allowed to evaporate slowly. After solvent treatment, the samples were investigated by both optical microscopy and scanning force microscopy (AFM). The AFM images were taken on a Digital Instruments Dimension 3100 microscope operated in tapping mode (free amplitude of the cantilever  $\approx 30$  nm, set point ratio  $\approx 0.98$ ). Film thicknesses were determined by purposely applying a scratch to the polymer film and subsequent AFM topography imaging in the vicinity of the scratch. Some of the samples were plasma-etched in an RF plasma (air  $\approx 2$  mbar) for different times to enable AFM imaging underneath the original surface of the film.

## Results and Discussion

**(a) Slow Drying Conditions.** We start our discussion with the samples prepared by spin coating, followed

\* Corresponding author. E-mail: georg.krausch@uni-bayreuth.de.

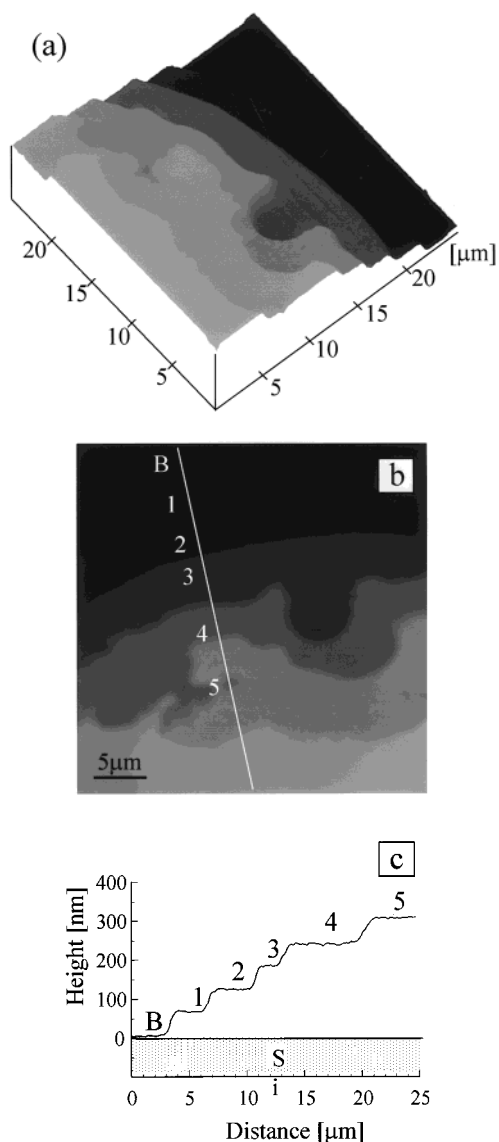


**Figure 1.** AFM topography image of a thin ABC block copolymer film after 3 week treatment in THF vapor. (a) 3D presentation of a stepped portion of the film surface near the edge of the sample. (b) Same image as that in part (a) in top view presentation. The letter and numbers (B and 1–5) are used to refer to areas of different height. (c) Cross section through the AFM image displayed in parts (a) and (b) along the white line indicated in part (b). The location of the silicon substrate (Si) is indicated for clarity.

by solvent vapor treatment and slow drying. As cast, the films appear laterally homogeneous in the optical micrographs. Accordingly, the film surfaces appear flat and featureless in the AFM topography images. On exposure to the vapors of chloroform, THF, and toluene, however, the surfaces develop areas of well-defined thicknesses. This effect is most pronounced in regions where the overall film thickness is laterally varying. Such regions are typically found near the edges of the specimen or close to defects such as dust particles, which are wet by the polymer film. As an example, Figure 1a shows an AFM image of a copolymer film (initial average thickness = 520 nm) exposed to THF vapor for 3 weeks. We have chosen an area where the local film thickness is increasing from top to bottom. The surface clearly exhibits a steplike morphology. Quantitative evaluation of the step heights can be performed by

taking cross sections through the AFM image (Figure 1b,c). From a set of cross sections taken at different positions of the sample, we find that the step height  $d$  is constant within the experimental error and amounts to  $d = 62 \pm 5$  nm.

As mentioned above, bulk pieces of the polymer prepared from THF solution exhibit a lamellar morphology.<sup>10</sup> This finding, together with the fact that we were unable to detect any lateral structure on top of the terraces, indicates that the step structure results from lamellae being aligned parallel to the plane of the film. This observation resembles the well-known surface-induced alignment found in thin films of symmetric diblock copolymers,<sup>7</sup> where the preferential attraction of the respective blocks to the confining boundary surfaces generally leads to an in-plane alignment of the lamellae. In the case of the particular triblock copolymer studied here, a parallel alignment of lamellae is surprising at first sight, as the polar 2VP middle block is expected to preferentially adsorb onto the (polar)  $\text{SiO}_x$  substrate. Indeed, recent experiments on ultrathin layers of a similar ABC triblock copolymer showed a laterally microphase-separated morphology possibly triggered by the preferential adsorption of the middle block<sup>12</sup> in agreement with recent theoretical predictions.<sup>13</sup>

To elucidate this somewhat puzzling situation, we have investigated in some detail the first layer of block copolymer, which is in intimate contact with the substrate surface. The thickness of this bottom layer of copolymer (denoted by "B" in Figure 1) was determined after applying a scratch to the polymer film prior to AFM imaging. Care has been taken to remove the polymer within the scratch without damaging the  $\text{SiO}_x$  substrate surface. Cross sections through AFM images taken across the scratch (Figure 2a,b) reveal that the bottom layer thickness amounts to only about 4 nm. Moreover, a high-resolution image of the bottom layer surface reveals a distinct lateral structure with a characteristic lateral spacing of some 60 nm. We note that quite similar surface morphologies can be created by dipping a clean substrate into a highly dilute solution of the same polymer and subsequently rinsing it in pure solvent (not shown here). We therefore conclude that the  $\text{SiO}_x$  substrate is covered by a thin layer of block copolymer via strong physisorption of the 2VP middle block as soon as the substrate is brought in contact with the copolymer solution during spin casting. This layer may best be described as a microphase-separated copolymer brush, which then acts as the actual substrate for microdomain alignment in thicker films. Indeed, it can be expected that the adsorption of this bottom layer leads to an effective reduction of the surface energy of the substrate. Moreover, as has been shown before,<sup>12</sup> all three blocks of the copolymer should be exposed at the surface of the adsorbed layer. In view of the relative volume fractions of PS and PtBMA, we may identify the protrusions in Figure 2c as PtBMA microdomains. Given that the lateral structure observed in the adsorbed layer does not coincide with lamellae oriented perpendicular to the plane of the film, it may be energetically more favorable to cover the brush surface with a continuous layer of the tBMA end block leading to the observed alignment of lamellae parallel to the substrate. As a matter of fact, in view of the surface energies of the three blocks, such parallel alignment should be preferred at the free surface of the polymer film as well.

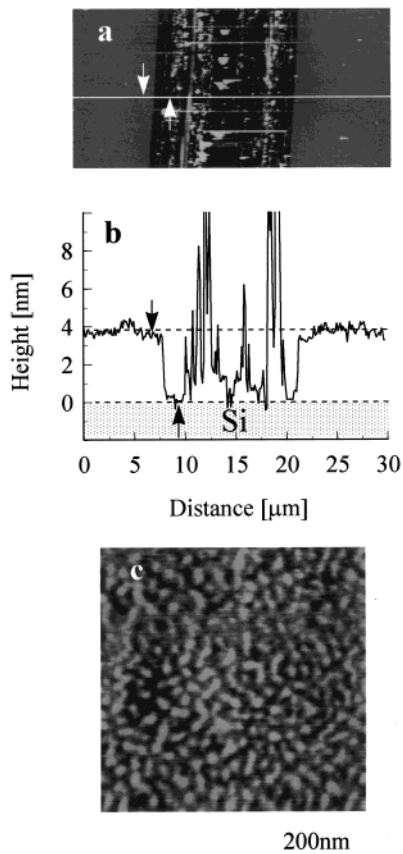


**Figure 2.** (a) AFM image of a scratch through layer B. The height scale ranges from 0 to 10 nm. (b) Cross section through the scratch displayed in part a. (c) Higher magnification image of the surface of layer B. The height scale ranges from 0 to 4 nm.

In the following, we shall concentrate on the microstructure in the vicinity of the steps between the bottom layer (B) and the first lamella. As an example, Figure 3a shows an AFM topography image of such an edge. The gray scale has been chosen so that the bottom layer (B) appears black, and the upper terrace (1) appears white, to reveal the surface morphology in the vicinity of the step with high enough height resolution. As is clearly seen in Figure 3a, the terrace edge is characterized by a well-defined pattern of parallel height corrugations oriented perpendicular to the step. The pattern has a characteristic lateral period of about 90 nm, the amplitude of the height modulations amounts to about 1 nm, and the pattern extends about 1  $\mu\text{m}$  from the step into the underlying terrace. Moreover, we find a long stripe of a similar pattern extending from the upper left of the AFM image along the diagonal toward the step. Again, a preferred orientation of the height corrugations along the diagonal (i.e., toward the step edge) is observed.

To interpret the above findings, it is instructive to envisage the large-scale morphological changes of the samples during the drying process. In the bottom part of Figure 3, we show two optical micrographs taken at the same spot of the sample during vapor treatment (Figure 3b) and after drying (Figure 3c). The two terraces are characterized by different colors due to white light interference. On drying, the film shrinks in both thickness and width. Whereas the former is revealed from a change in the interference colors, the lateral shrinkage results in a retraction of the step edges

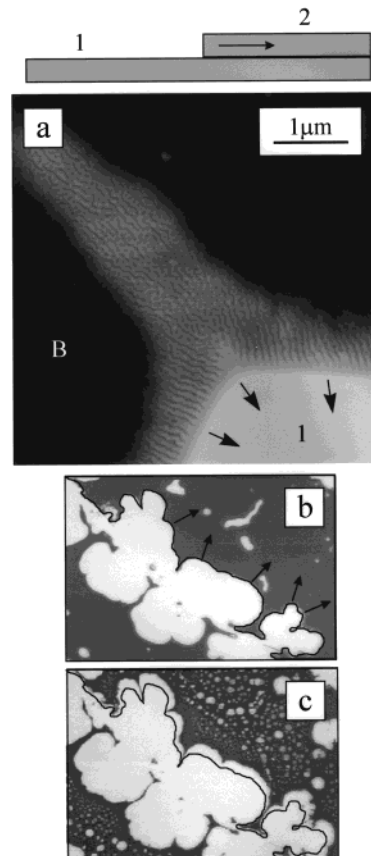


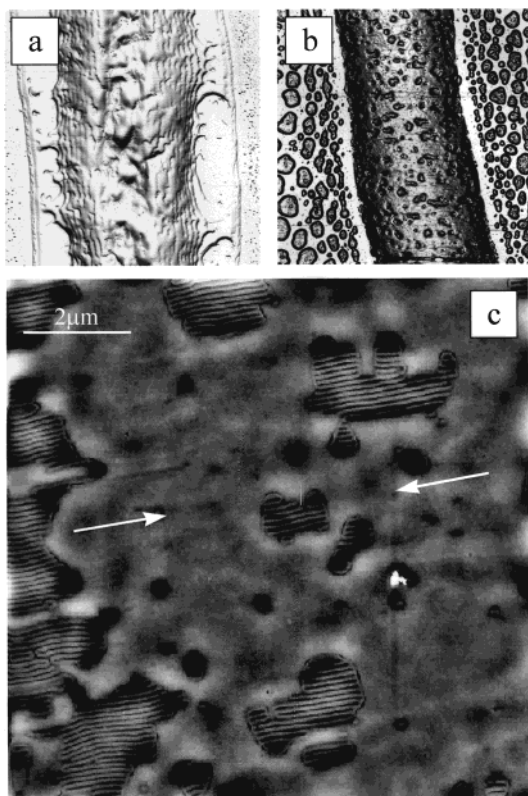
**Figure 3.** (a) AFM topography image (tapping mode) of a thin film of the polymer after treatment in THF vapor, followed by slow removal of the solvent. The gray scale has been chosen such that the small height corrugations in the vicinity of the step become visible. No lateral structure is observed in the flat area indicated by 1 (first lamella). The amplitude of the height corrugations around the step edge amount to about 1 nm. (parts b and c) Optical micrographs of the same sample in the vicinity of a scratch running from top left to bottom right ( $420 \times 300 \mu\text{m}^2$ ). The same spot has been imaged in situ during THF exposure (part b) and after drying (part c). The different gray values correspond to white light interference colors. The arrows in part b indicate the retraction of the lamellar edge on drying. For clarity, the location of one of the edges before drying has been marked by a black line (part b), which is superimposed on the optical micrograph taken after drying (part c) for comparison.

as indicated by the arrows in Figure 3b. In addition, holes are formed in the upper terrace. The retraction of the step edges obviously leads to a mechanical strain field between the first lamella and the underlying, strongly absorbed bottom layer. We may assume as a working hypothesis that the lateral structures observed in the vicinity of the step edges result from an alignment of the lamellae induced by this strain field during the drying process.

Before we discuss the effects of drying in more detail below, we note explicitly that we shall exclude a detailed quantitative investigation of the observed characteristic spacings from the present discussion. Indeed, the characteristic lengths (step heights and lateral spacings) are found to depend in a complex manner on molecular weight, solvent quality, and the details of the preparation procedure. A comprehensive experimental study of these effects is presently under way and will be published elsewhere.<sup>14</sup>

**(b) Fast Drying.** To test the above hypothesis of the role of mechanical strain fields during drying, it is

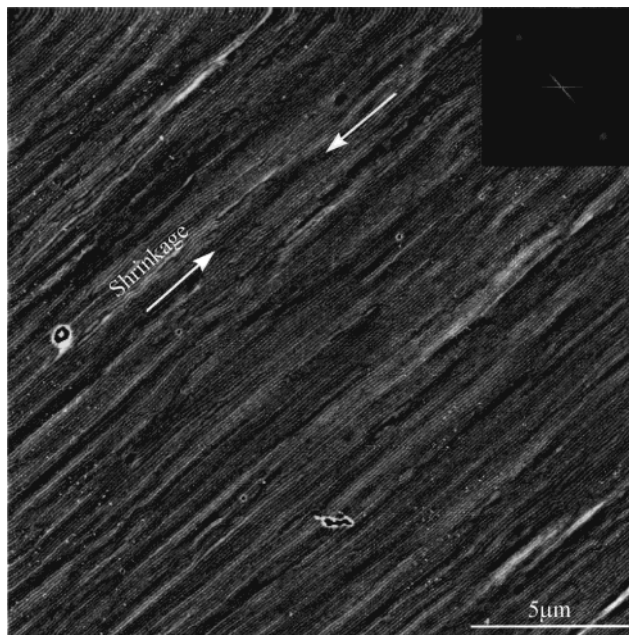




**Figure 4.** AFM topography images of stripes of triblock copolymer after slow (a) and rapid (b) removal of THF vapor. The size of the images is  $100 \times 100 \mu\text{m}^2$ . (c) Close up of part of the area shown in part b. The height scale ranges from 0 to 5 nm. The white arrows indicate the direction perpendicular to the long axis of the stripe.

instructive to study faster drying conditions, where stronger mechanical fields are to be expected. Moreover, to simplify data interpretation, we have chosen sample geometries, where mechanical strain fields occur in a highly anisotropic manner. The latter can be achieved when narrow stripes of the block copolymer are exposed to the solvent vapor treatment. Here, lateral shrinkage is expected to occur predominantly along the direction perpendicular to the long axis of the stripe, and the strain fields should be limited predominately to the plane perpendicular to the long axis of the stripe. Narrow stripes are readily formed when the block copolymer solution is placed between two solid walls during film preparation. After solvent evaporation, one is eventually left with a set of interconnected rims of block copolymer. In our case, such rims are typically  $0.3\text{--}1 \mu\text{m}$  thick, some  $1\text{--}50 \mu\text{m}$  wide, and several millimeters long. When exposed to a solvent vapor, such structures will expand in height and width, but expansion along the stripe is hardly possible. Accordingly, on solvent removal, shrinkage is expected to occur predominantly along the same axes.

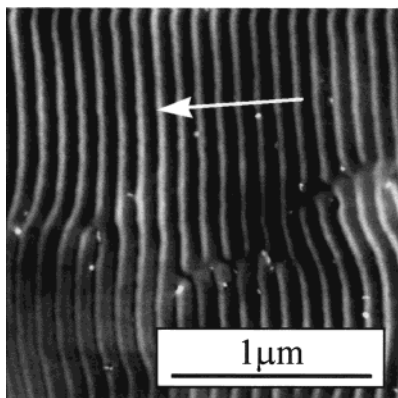
Figure 4 shows AFM images of a  $38 \mu\text{m}$  wide and  $550 \text{ nm}$  thick copolymer stripe after swelling in THF vapor and subsequent drying. In agreement with the above experiments, slow solvent removal (Figure 4a) leaves a stepped polymer surface indicative of an alignment of the lamellae parallel to the plane of the film. The large-scale morphology clearly shows that the polymer stripe has shrunk perpendicular to its long axis. At some points, the lowest lamella seems to have been pinned at some defects during retraction. We note that more than eight successive lamellae can be observed, indicat-



**Figure 5.** AFM topography image of the triblock copolymer stripe after treatment in chloroform and fast drying. The height scale ranges between 0 and 5 nm. The white arrows indicate the directions perpendicular to the long axis of the stripe. A Fourier transform of the image is shown in the inset.

ing a strong surface-induced ordering of the block copolymer film. A completely different surface morphology is observed after fast solvent removal. As can be seen in Figure 4b, the polymer stripe exhibits a smooth and rounded surface. No steps are observed. In contrast, the surface of the stripe exhibits isolated areas with a distinctly different surface morphology. This is shown in Figure 4c, where a smaller portion on the stripe surface has been imaged with higher lateral resolution. The AFM topography image clearly reveals a well-defined surface morphology within these areas. With the white arrows indicating the direction perpendicular to the long axis of the stripe, a well-defined height corrugation pattern oriented along the dominant lateral shrinkage direction is observed. The structure is similar to the one observed in Figure 3a. However, the orientation of the lateral corrugations is the same for the entire area displayed in Figure 4b and is determined by the macroscopic morphology of the polymer specimen. We conclude at this point that a shrinkage-induced alignment of the lamellae during the drying process is again responsible for the observed surface structure.

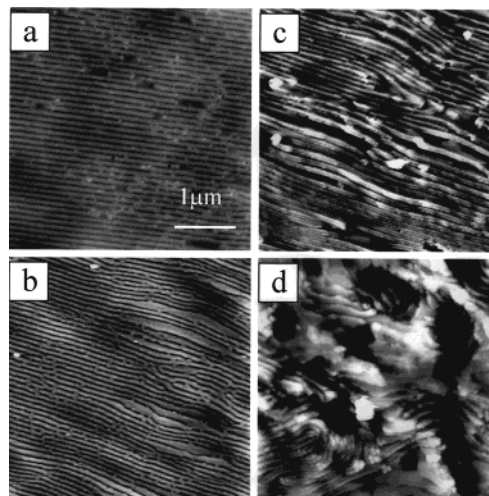
It is interesting to note that under somewhat different conditions an even better microdomain alignment can be observed. Figure 5 shows the surface area of a similar stripe after exposure to chloroform vapor and subsequent fast solvent removal. Chloroform has a slightly higher vapor pressure than THF and therefore is expected to enable faster solvent extraction. Indeed, after treatment of a block copolymer stripe in chloroform vapor and fast solvent removal, the entire polymer surface exhibits a well-oriented corrugation pattern. In Figure 5, a  $20 \times 20 \mu\text{m}^2$  area of the block copolymer film is shown. Again, the dominant lateral shrinkage direction is indicated by white arrows. In the inset to Figure 5, a 2D Fourier transform of the AFM image is shown, clearly revealing two distinct peaks located at  $q = 0.097 \pm 0.02 \text{ nm}^{-1}$ , corresponding to a lateral periodicity of  $65 \pm 2 \text{ nm}$ .



**Figure 6.** AFM topography image of a triblock copolymer stripe after exposure to toluene vapor and subsequent fast solvent removal. The white arrows indicate the direction perpendicular to the long axis of the stripe. The height scale ranges between 0 and 5 nm.

In addition to the alignment of the lamellae along the direction *perpendicular* to the long axis of the stripes discussed above, alignment of the lamellae *along* the long axis of the stripe is observed in some cases, too. As an example, Figure 6 shows the surface morphology of a copolymer stripe after exposure to toluene vapor and subsequent fast solvent removal. Again, a highly oriented lamellar morphology is found; however, the lamellae are oriented along the long axis of the copolymer stripe. Similar results have been obtained for considerably narrower polymer stripes after exposure to chloroform vapor as well.

Before we discuss the above results in more detail, we shall point to a shortcoming of the AFM experiments presented so far. As AFM is only sensitive to the surface morphology of the specimens, one might ask how far the order evident at the surface extends into the "bulk" of the copolymer stripe. Because of the particular sample geometry, cross-sectional transmission electron microscopy experiments are prohibitively tedious. Up to now, we have not been able to characterize our samples using cross-sectional TEM. As an alternative, we exposed the highly oriented samples to an RF plasma to erode parts of the sample. The experimental conditions were chosen such that about 100 nm of the block copolymer was removed during each etching step. After each step, AFM images were taken at about the same position of the sample. The result of this procedure is shown in Figure 7. We find that the domain alignment observed at the free surface of the film (Figure 7a) is still visible some 100 (Figure 7b) and 200 nm (Figure 7c) below the original surface of the sample. Figure 7c still exhibits a quite anisotropic domain morphology; however, the overall roughness of the sample has increased during the plasma treatment and several large defects become visible. After continued plasma treatment, the AFM images eventually are dominated by the defect structure and a large surface roughness. Figure 7d shows the specimen after some 600 nm have been removed. In Figure 7d, we are no longer able to detect any preferential orientation of the domains. It must be noted though that the extent of roughness created by the plasma treatment points to the limits of this experimental approach and renders a quantitative interpretation of the results impossible. With the experimental evidence available at present, we can only conclude that the alignment of the domains extends over some 100 nm into the films. If we do accept the AFM image of



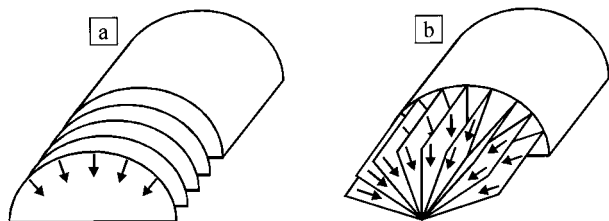
**Figure 7.** AFM topography images of a triblock copolymer stripe treated as in Figure 3 before (a) and after removing the top 100 (b), 200 (c), and 600 nm (d) of the sample in an RF plasma. The height scale ranges from 0 to 10 nm in all images.

Figure 7d at face value, we conclude that most of the alignment is lost deep within the sample. This finding indicates that the mechanical strain fields are larger at the physical surface of the film as compared to the regions close to the substrate. However, further experimental evidence will be needed to establish the overall morphology of the specimens in full detail.

**(c) Discussion.** The experimental results can be summarized as follows. Slow solvent evaporation conditions result in an effective alignment of the lamellae within the plane of the film. Fast solvent evaporation conditions, on the other hand, lead to a lamellar orientation perpendicular to the plane of the film. Samples with a stripelike shape exhibit two preferred lateral orientations of the lamellae, i.e., along and perpendicular to the long axis of the stripe. Although we are unable at present to clearly identify the conditions under which one of the two lateral orientations is realized, we observe a clear correlation between the lamellar orientation and the macroscopic anisotropy of the polymer specimen. This correlation can be used to create large monodomains.

At first sight, our experiments resemble recent investigations on the influence of the solvent extraction speed on the morphology of poly(styrene-*b*-butadiene-*b*-styrene) (SBS) triblock copolymer thin films prepared from solution.<sup>3,4</sup> The authors reported a rather disordered morphology at high solvent extraction rates, cylinders oriented perpendicularly to the plane of the film for intermediate extraction rates, and a parallel orientation of cylinders at low solvent extraction rates. Similarly, for the case of lamellar PS-PB diblock copolymers, an alignment of the lamellae perpendicular to the plane of the film was observed under fast solvent extraction conditions.<sup>15</sup> The findings were explained by a higher diffusivity of the solvent in the PB microdomains. Obviously, a perpendicular orientation of cylinders/lamellae in the film allows faster solvent transport to the film surface, which is favored under fast solvent extraction conditions. Under slow solvent extraction conditions, the system was able to reach a morphology close to the melt equilibrium, i.e., a parallel alignment of the cylinders/lamellae within the plane of the film. These effects may indeed be partially responsible for the observed alignment of the microdomains





**Figure 8.** Sketch of two possible lamellar orientations allowing the copolymer chains to move within a single lamella during shrinkage. The two scenarios relate to the observed surface structure shown in Figures 3, 4a, and 6b, respectively.

observed in our experiments. However, we need to realize some significant differences to the solvent casting studies discussed above. In contrast to the situation of a film quickly dried from solution, in our experiments, the initial morphology is a well-ordered, microphase-separated structure. This is clearly revealed by the optical micrographs taken before solvent removal (Figure 3b). Moreover, in our experiments, the fastest solvent extraction rates were found to produce a perfectly ordered microdomain morphology. Finally, the long-range alignment of the lamellae with respect to the macroscopic shape of the specimen cannot be explained by the model previously proposed.<sup>3,4</sup>

It is illuminating also to consider the effect of mechanical strain fields accompanying the shrinkage process during solvent removal. Figure 3b (taken under solvent atmosphere) indicates that the drying process of the polymer stripes starts from a stack of swollen lamellae aligned parallel to the plane of the film. On slow solvent removal, we can assume a successively decreasing but spatially homogeneous solvent concentration throughout the entire stack of lamellae. Consequently, all lamellae are expected to shrink at about the same rate, and hardly any shear should occur between neighboring lamellae. The situation may be somewhat more complex in the vicinity of the substrate, as the lateral shrinkage of the bottom layer is hindered by substrate interactions. Indeed, the effect shown in Figure 3a indicates a strong interaction between the bottom layer and the first lamella and may well be explained by a shearing motion between the two. High solvent extraction rates, on the other hand, will lead to a fast shrinkage of the polymer stripe. The overall shape of the stripe after fast drying (Figure 4b) resembles a cylindrical cap. For geometrical reasons, the dominant movement of polymer chains during the shrinkage process is directed toward the center of the cylinder, and chains will predominantly move in directions perpendicular to the cylindrical axis. A preferential alignment of the lamellae along planes including these directions would enable the copolymer chains to move within the plane of the interface (i.e., without crossing different lamellae) during shrinkage. In Figure 8, we sketch two possible lamellar orientations that are compatible with this notion. In Figure 8a, lamellae are oriented perpendicularly both to the surface and to the long axis of the cylinder. Any movement of copolymer chains during shrinkage can be accommodated within these planes. Similarly, Figure 8b shows an alternative lamellar orientation, where chain motion during shrinkage can be realized without crossing between neighboring planes. Both lamellar orientations will result in the lateral structures observed in the above experiments.

It is tempting to compare our results to recent studies of the effect of external mechanical fields on the align-

ment of block copolymer microdomains.<sup>16</sup> Our results to some extent resemble shear experiments on diblock copolymer melts, where depending on shear rates and amplitudes, different orientations of the lamellae with respect to the direction of the mechanical fields can be induced.<sup>17–20</sup> The different scenarios discussed above relate to what is called the *parallel orientation* (at low solvent extraction rates) and the *perpendicular and transverse orientations* (after fast solvent removal). The stability of the original parallel orientation of the lamellae with respect to the plane of the film (and therefore the shear plane) during slow solvent extraction is in qualitative agreement with the results reported by Koppi et al.<sup>18</sup> for PEP-*b*-PEE diblock copolymers and by Wiesner<sup>17</sup> for PS-*b*-PI diblock copolymers exposed to large-amplitude oscillatory shear. In both cases, parallel orientation of the lamellae with respect to the shear plane was induced at low shear rates, and the perpendicular orientation occurred at higher shear rates. Although a detailed understanding of this transition is still lacking, a destruction and reorganization mechanism was suggested,<sup>18,20</sup> which leads to an alignment of the lamellar director perpendicular both to the shear direction and the direction of the shear gradient. Again, a preferred motion of block copolymer molecules within the lamellae was discussed as a possible microscopic origin of the observed alignment effects. We are aware of the differences between an oscillatory shear experiment performed on a block copolymer melt and the experimental situation during solvent removal from a block copolymer thin film. However, the strong influence of the mechanical strain fields present during shrinkage and the observed microdomain alignment lead us to the conclusion that similar underlying processes may be responsible.

We finally turn to the differences in surface morphology observed after fast drying from THF (Figure 4c) and chloroform (Figure 5). After THF treatment, only a small portion of the surface area exhibits the perpendicular orientation of lamellae, whereas a large part of the surface appears rather flat and featureless in the AFM images. This observation may be understood in terms of the surface energy differences between the three blocks. After solvent removal, it will be energetically favorable to cover the free surface of the triblock copolymer film by a continuous layer of one of the lower surface energy components (i.e., one of the outer blocks). The formation of a continuous top layer of the lower surface energy component even in the case of an overall perpendicular orientation of the lamellae was observed in the early days of cross-sectional TEM on diblock copolymer thin films.<sup>21</sup> We may assume that the entire sample has been aligned during drying; however, large parts of the surface were subsequently covered by a thin homogeneous layer, exposing one of the outer blocks to the free surface of the film. In the case of chloroform, however, the faster evaporation may have prevented the formation of a homogeneous top layer, thereby freezing in a highly nonequilibrium surface morphology.<sup>15</sup>

## Conclusion

In summary, we have shown that the thin film morphology of ABC triblock copolymer films depends crucially on the preparation conditions. Exposure to solvent vapors followed by slow solvent removal leads to strong surface-induced alignment of lamellae within the plane of the film. The spontaneous adsorption of a laterally microphase-separated brush layer at the polar

substrate was suggested to explain the observed surface-induced lamellar alignment. Fast solvent vapor extraction lead to perpendicular alignment of the lamellae with respect to the plane of the film. In addition, a high degree of lateral order could be induced by use of macroscopically anisotropic specimens. The results are in qualitative agreement with recent experiments on shear alignment of diblock copolymer melts. We note that, at present, the parameters characterizing the swelling and drying processes are only poorly controlled, thereby rendering a systematic study of the proposed effects rather difficult. Further work will have to concentrate on the proper experimental setups that allow for the control of temperature, vapor pressure, and vapor extraction speed. As drying from solution is a quite common technique to achieve "equilibrium" morphologies of complex block copolymers, a sound understanding of the effects occurring on drying seems quite important.

**Acknowledgment.** We thank R. Stadler (deceased) and E. Giebler for synthesis and bulk characterization of the ABC triblock copolymer. We acknowledge helpful discussions with V. Abetz and M. Geoghegan during the preparation of the manuscript. The authors appreciate financial support through the Deutsche Forschungsgemeinschaft (KR1369/9 and SFB 481).

#### References and Notes

- (1) Bates, F. S.; Frederickson, G. H. *Annu. Rev. Phys. Chem.* **1990**, *41*, 525.

- (2) For a recent review, see: Bates, F. S.; Frederickson, G. H. *Physics Today* **1999**, *52*, 32.
- (3) Kim, G.; Libera, M. *Macromolecules* **1998**, *31*, 2569.
- (4) Kim, G.; Libera, M. *Macromolecules* **1998**, *31*, 2670.
- (5) Albalak, R. J.; Capel, M. S.; Thomas, E. L. *Polymer* **1998**, *39*, 1647.
- (6) Goldacker, T.; Abetz, V.; Stadler, R.; Erukhimovich, I. Y.; Leibler, L. *Nature* **1999**, *398*, 137.
- (7) Anastasiadis, S. H.; Russell, T. P.; Satija, S. K.; Majkrzak, C. F. *Phys. Rev. Lett.* **1989**, *62*, 1852.
- (8) Krausch, G. *Mater. Sci. Eng. Rep.* **1995**, *14*, 1.
- (9) Giebler, E.; Stadler, R. *Macromol. Chem. Phys.* **1997**, *198*, 3815.
- (10) Giebler, E. Dissertation, Universität Mainz, 1997.
- (11) Reiter, G. *Phys. Rev. Lett.* **1992**, *68*, 75.
- (12) Elbs, H.; Fukunaga, K.; Stadler, R.; Magerle, R.; Krausch, G. *Macromolecules* **1999**, *32*, 1204.
- (13) Pickett, G. T.; Balazs, A. C. *Macromol. Theory Simul.* **1998**, *7*, 249.
- (14) Elbs, H.; Fukunaga, K.; Magerle, R.; Krausch, G. 1999, to be published.
- (15) Turturro, A.; Gattiglia, E.; Vacca, P.; Viola, G. T. *Polymer* **1995**, *36*, 3987.
- (16) Honeker, C. C.; Thomas, E. L. *Chem. Mater.* **1996**, *8*, 1702.
- (17) Wiesner, U. *Macromol. Chem. Phys.* **1997**, *198*, 3319.
- (18) Koppi, K. A.; Tirell, M.; Bates, F. S.; Almdal, K.; Colby, R. H. *J. Phys. II* **1992**, *2*, 1941.
- (19) Winey, K. I.; Patel, S. S.; Larson, R. G.; Watanabe, H. *Macromolecules* **1993**, *26*, 2542.
- (20) Hadzjioannou, G.; Mathis, A.; Skoulios, A. *Colloid Polym. Sci.* **1979**, *257*, 136.
- (21) Hasgawa, H.; Hashimoto, T. *Macromolecules* **1985**, *18*, 589.

MA9910639